Vol. 734: 91–104, 2024
https://doi.org/10.3354/meps14555

MARINE ECOLOGY PROGRESS SERIES
Mar Ecol Prog Ser

Published April 18

Age validation of yellowfin tuna *Thunnus albacares* in the Indian Ocean using post-peak bomb radiocarbon chronologies

Igaratza Fraile[1,*], Patricia L. Luque[1], Steven E. Campana[2], Jessica H. Farley[3], Kyne Krusic-Golub[4], Naomi Clear[3], J. Paige Eveson[3], Iraide Artetxe-Arrate[1], Iker Zudaire[1], Hilario Murua[5], Gorka Merino[1]

[1]AZTI, Marine Research, Basque Research and Technology Alliance (BRTA), Pasaia, Gipuzkoa 20110, Spain
[2]Faculty of Life and Environmental Sciences, University of Iceland, Reykjavik 102, Iceland
[3]CSIRO Environment, Hobart, Tasmania 7000, Australia
[4]Fish Ageing Services, Queenscliff, Victoria 3225, Australia
[5]International Seafood Sustainability Foundation, 3706 Butler Street, Pittsburgh, PA 15201, USA

ABSTRACT: Yellowfin tuna *Thunnus albacares* stock assessments use age-structured models; therefore, accurate methods for ageing the catch are required. Age estimation techniques need to be validated at the population level to ensure accuracy. However, otolith-based age estimates of yellowfin tuna have never been validated in the Indian Ocean. The current study provides the first age validation for Indian Ocean yellowfin tuna using the post-peak decline period of the bomb radiocarbon (^{14}C) chronometer. A ^{14}C reference chronology based on accelerator mass spectrometry assays of known-age yellowfin tuna otoliths was consistent with published regional coral records, with all showing similar rates of decline during the 2000 to 2019 study period. After back-calculating the birth years of sub-adult and adult yellowfin tuna from otolith increment counts, $\Delta^{14}C$ values measured in the early growth portion of the otolith were compared with the observed decline slope of the reference chronology. There were no significant differences between the birth years of validation and reference samples, supporting the otolith increment age determination methodology between the ages of 2.2 and 10.5 yr. The validation of age and growth estimates is expected to benefit assessment models for Indian Ocean yellowfin tuna. We recommend that otoliths from large fish continue to be collected to expand the validation to older fish. Greater precision in the validation results will also require a larger reference chronology.

KEY WORDS: Bomb radiocarbon · Carbon-14 · Yellowfin tuna · Otolith chemistry · Age validation

1. INTRODUCTION

Yellowfin tuna *Thunnus albacares* is an economically important pelagic species inhabiting tropical and subtropical waters of the world's 3 major oceans. This valuable species is heavily exploited by both artisanal and industrial fisheries operating around the globe (FAO 2020, Artetxe-Arrate et al. 2021). In 2021, total catches of yellowfin tuna in the Indian Ocean were close to 415 000 Mt, accounting for 9% of major commercial global tuna catches (IOTC 2023, ISSF 2023). Given such intense fishing pressure, a good understanding of the species' biological processes, such as age, growth, and mortality, is required to ensure a correct evaluation of the population and effective management of the resource.

Age estimation of fish is a key area of research in fisheries science, since most population dynamics

*Corresponding author: ifraile@azti.es

models used to assess the status of a stock are dependent on age-based parameters. Fish age estimates are often obtained counting paired opaque and translucent bands in calcified structures, such as otoliths (Campana 2001). Commonly used methods to estimate age and/or growth include tagging studies (determining the change in size of individuals between the time of tagging and recapture), analysis of length-frequency data (length-frequency distribution of the catches generally exhibit modes that can be tracked over time, although this is generally restricted to small/young fish), and the study of calcified structures (counting daily and/or annual growth zones in otoliths, fin spines, or vertebrae), among others (Campana 2001). Otoliths are the preferred hard structures for ageing studies in tuna due to their metabolically inert formation, which prevents resorption, unlike other structures like fin spines and scales that lead to age underestimation of older individuals (Lessa & Duarte-Neto 2004). As a result, otoliths can provide accurate age estimates over a broad age range (e.g. Eveson et al. 2015, Sardenne et al. 2015, Farley et al. 2020). During otolith formation, rhythmic/seasonal variations in the deposition rate of calcium carbonate results in the creation of alternating opaque and translucent zones that can be interpreted as annual growth increments or daily micro-increments (Morales-Nin 2000), although the physiological mechanisms behind increment formation are not fully understood (Kalish 1989, Campana 1999). In addition, maximum age is key for estimating natural mortality, which in turn is one of the most influential parameters in stock assessment models (Then et al. 2015, Punt et al. 2021).

Although the age and growth of yellowfin tuna have been widely investigated, different growth rates have been reported for different stocks and even for different areas within a stock, leading to uncertainties in terms of age validation and maximum age (Murua et al. 2017). Discrepancies in growth parameters among studies are often derived from the ageing criteria applied by different laboratories and/or readers, although the lack of a proper sampling design is also a common source of uncertainty, due partly to the selectivity of the fisheries that makes it difficult to collect representative samples of the whole population (Murua et al. 2017, Lu et al. 2023). Counting annual growth increments in the otoliths of tropical tuna, such as yellowfin, has been challenging because the increments are often difficult to identify (Farley et al. 2020, Pacicco et al. 2021). As stock status indicators are heavily influenced by fish growth, extensive research efforts have been made over recent years to improve direct daily and annual age estimation methods for yellowfin tuna. Farley et al. (2020) developed a novel method to calculate the fractional (decimal) age of yellowfin tuna in the Pacific Ocean, combining counts of daily and annual increments in otoliths. This age determination method was recently applied to yellowfin tuna in the Indian Ocean (Farley et al. 2021). The maximum age calculated for yellowfin tuna from the Indian Ocean using this method was at least 10.9 yr, somewhat older than previous reported values around 9.5 yr (Shih et al. 2014).

Age estimates need to be validated for each species and even for different stocks of the same species (Campana 2001). However, otolith age estimates for yellowfin tuna in the Indian Ocean have not yet been validated. Several techniques are used to validate age estimates such as the analysis of otoliths from mark–recapture of chemically tagged wild fish (e.g. Krusic-Golub & Ailloud 2022), individuals reared in captivity (e.g. Ticina et al. 2007), and radiometry (lead–radium dating, e.g. Andrews et al. 2011a) or bomb radiocarbon dating of otoliths (Campana 2001).

While age validation of yellowfin tuna has been conducted for the larval stages in the Pacific Ocean (Wexler et al. 2001) and more recently for adults in the Atlantic and Pacific Oceans (Andrews et al. 2020, Farley et al. 2020, Krusic-Golub & Ailloud 2022), studies that validate the age estimation of yellowfin tuna from the Indian Ocean across different age classes are scarce. Sardenne et al. (2015) demonstrated daily micro-increment formation in otoliths of yellowfin tuna from the Indian Ocean based on oxytetracycline mark–recapture experiments; however, the maximum time at liberty of the experiment was 3 yr, and yellowfin tuna were all less than 5 yr old, limiting the time-period of the validation.

The use of bomb radiocarbon (^{14}C) to validate otolith ages has proven to be an effective technique in fisheries biology (Kalish 1993). This approach recognizes that the atmospheric ^{14}C produced during nuclear bomb testing through the 1950s and 1960s was incorporated into marine waters and subsequently into biological calcified structures of marine organisms (e.g. otoliths, shells, corals) (Campana 1999). Since otolith-deposited material is not reabsorbed during the lifetime of a fish, ^{14}C leaves a detectable trace in the otolith at the time of deposition (Kalish 1993). After the nuclear test ban treaty in 1963, ^{14}C levels in oceanic carbonates continued to increase in the next decade to a peak of variable timing and amplitude (Nydal & Lovseth 1983, Guilderson et al. 2000, Mahadevan 2001). From the ~1980s onward, upper-ocean ^{14}C levels have been continu-

ously declining, but remain elevated relative to pre-1950s levels (Broecker & Peng 1982). The increase in bomb-produced ^{14}C levels was first described in hermatypic corals in Florida (Druffel & Linick 1978), and it has been shown that ^{14}C records in otoliths of shallow-water organisms are synchronous with the coral time-series (Kalish 1993, Campana 1997).

The change in bomb ^{14}C levels in reference chronologies (usually corals) has been used to confirm age estimates in several fish species (e.g. Kalish et al. 1997, Campana & Jones 1998, Campana 2001, Campana et al. 2002, Kastelle et al. 2008, 2020). The method is based on a comparison of ^{14}C values in the otolith core portion of aged fish with the equivalent year from a suitable and known-age reference ^{14}C time-series. The precision of the ^{14}C method depends on the position of the presumed birth year relative to the period of increasing or declining bomb ^{14}C concentrations, as well as the availability of a suitable reference chronology. The method is most precise for fish born during the steep increasing portion of the bomb curve (during the 1960s) where there is less chronological uncertainty in the ^{14}C concentrations (± ~2 yr), and most studies have validated the estimated ages of fish born during this period (e.g. Kalish et al. 1996, Campana 1997, Melvin & Campana 2010). As the ambient ^{14}C level flattens, the uncertainty increases. However, several studies have successfully used the gradual decline period of the bomb curve for validating age estimates of fish born in more recent years (Andrews et al. 2011b, 2015, 2018, DeMartini et al. 2018, Sanchez et al. 2019, Shervette et al. 2021), including studies of tuna and billfish (Ishihara et al. 2017, Andrews et al. 2020). The characteristics of the decline in ^{14}C vary regionally, much more so than the period of increase, and are influenced by spatial and temporal variations in atmospheric circulation and mixing with deeper waters (Druffel & Suess 1983, Michel & Linick 1985, Grumet et al. 2005, Gao et al. 2021). Recently, Raj et al. (2022) presented a compilation of ^{14}C records in corals from different regions of the Indian Ocean, which is a useful reference for ^{14}C ageing studies in the Indian Ocean.

An age validation study using post-peak bomb radiocarbon dating has been recently completed for yellowfin tuna from the Atlantic Ocean (Andrews et al. 2020) and from the western and central Pacific Ocean (Andrews et al. 2022). The current study presents the first application of the post-peak bomb ^{14}C age validation method to test the validity of annual age estimates of yellowfin tuna in the Indian Ocean. First, a coral chronology from the north-central Indian Ocean (Raj et al. 2022) during the post-peak decline period was combined with known-age yellowfin tuna otolith measurements to form a ^{14}C reference chronology suitable for our study. Then, ^{14}C assays of sub-adult and adult yellowfin tuna otoliths with birth years between 2004 and 2018 based on the age determination method used by Farley et al. (2021) were compared with this reference chronology. Finally, ^{14}C-derived ages and direct age estimates of the same fish were compared to assess the validity of ages estimated from annual growth increment counts.

2. MATERIALS AND METHODS

2.1. Sample collection and selection

Sagittal otoliths from yellowfin tuna were collected in the western Indian Ocean between 2006 and 2020 (Fig. 1). Straight fork length (SFL) was measured to the nearest cm for all fish. Otoliths were extracted from fresh fish using forceps, carefully cleaned of

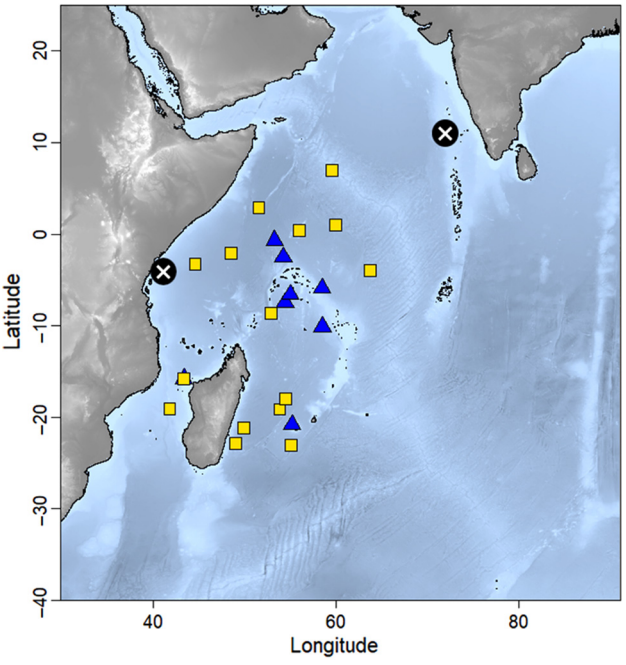

Fig. 1. Sampling locations of yellowfin tuna *Thunnus albacares* otoliths in the western Indian Ocean. Points in the map represent known-age tuna (age-0 and age-1) used as reference chronologies (blue triangles) and age-2+ tuna used for age validation (yellow squares). Two coral $\Delta^{14}C$ records were compared with otolith data: Watamu coral record, in the western Indian Ocean (Grumet et al. 2002), and Kadmat Island in the northern Indian Ocean (Raj & Bhushan 2021), which are marked with black open circles enclosing a cross. The latter was used in combination with otoliths of yellowfin tuna as a reference chronology

adhering organic tissue, and stored dry in polyethylene vials before subsequent analysis. Based on the SFL measurements, otoliths from 17 age-0 and age-1 yellowfin tuna were selected for the reference chronology, and otoliths from 30 sub-adult and adult fish (SFL >100 cm) for which both otoliths were available were selected for age validation (Fig. 1). One otolith from each of the 30 pairs was randomly selected for ^{14}C analysis, and the second otolith was used for direct age estimation based on annual growth increment counts. The known-age reference set was composed of otoliths from fish with SFL <60 cm, estimated to be of age 0 or 1 based on daily micro-increment counting (Farley et al. 2021), and birth years ranging from 2006 to 2019. Otoliths for age validation were selected based on an individual's SFL and catch date with the objective of selecting tuna from cohorts throughout the post-peak decline period. The SFL of sub-adult and adult yellowfin tuna was between 103 and 171 cm, and assumed birth years after back-calculating the estimated otolith age (see Section 3) from the catch date ranged from 2005 to 2018.

2.2. Otolith preparation and age estimation

Otoliths used for age estimation were sent to Fish Ageing Services (Queenscliff, Australia; www.fishageingservices.com) where they were prepared for annual age readings based on the method recently developed for yellowfin tuna in the Indian Ocean (Farley et al. 2021). Otoliths were embedded in rows of 5 in clear polyester resin and left to harden for a minimum of 24 h. Four serial transverse sections of approximately 320 µm thick were cut through the center of each otolith using a GEMMASTER slab saw equipped with an ultrathin diamond wafering blade (Pro-Slicer 4 × 0.004 × 5/8) to ensure that the nucleus of the otolith was included in at least 1 of the 4 sections (Fig. 2A). Sections were cleaned, dried, mounted onto glass microscope slides with further polyester resin, and covered with coverslips. All otolith preparations were examined using transmitted light with a LeicaM125 stereo microscope set at 25× magnification, and for each sample, the section that either contained the nucleus or cut closest to the nucleus was selected for ageing. Images of the sections were captured with a digital camera (The Imaging Source) attached to the microscope including a scale bar of 1 mm and analyzed with the camera's corresponding image analysis software (IC Measure, The Imaging Source ©). The position of the start of each opaque zone was marked, and the corresponding increment width (including the incomplete annuli width at the otolith edge) was measured (Fig. 2B). Decimal age of each fish was calculated following the method described by Farley et al. (2021). First, the age when the first opaque zone was completed was calculated using the relationship between daily age and otolith size (distance from the nucleus to the edge of the otolith) for paired otoliths. Then, the number of complete annual increments (opaque + translucent band) was counted. Finally, the time elapsed after the last opaque zone was deposited was estimated by comparing the size of the marginal increment with the mean size of marginal increments in all otoliths of the

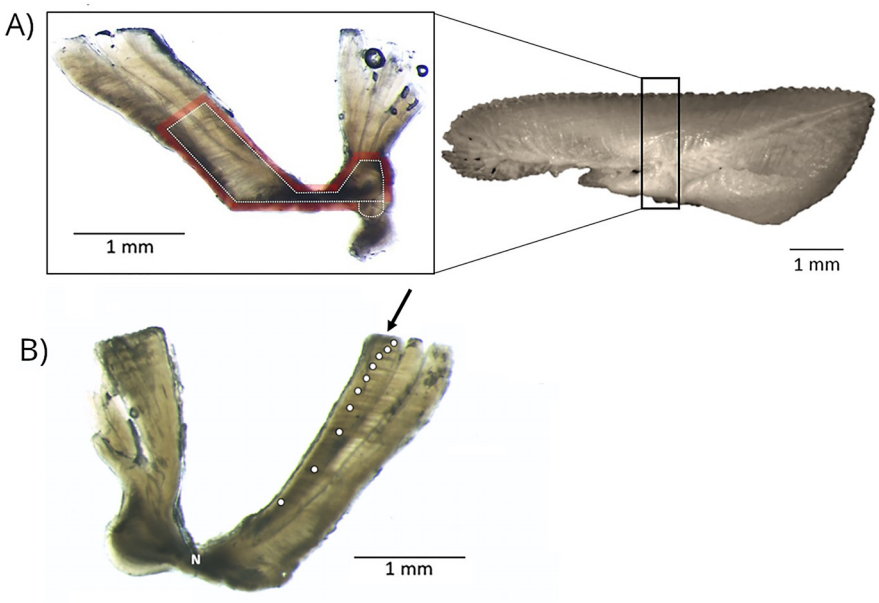

Fig. 2. (A) Photograph of a whole (right) sagittal otolith of an adult yellowfin tuna *Thunnus albacares* showing the slice selected for the transverse section containing the nucleus. Transverse section of the same yellowfin tuna (left), depicting the red shaded drilling path, which was used to extract the targeted early growth portion (dashed line) with a Micro-Mill precision drilling instrument. (B) Annual growth increments (white dots) in a transversely sectioned otolith from an Indian Ocean yellowfin tuna captured on 30 September 2021 (170.5 cm straight fork length). 'N' indicates the position of the nucleus. The increment on the otolith edge (black arrow) is considered incomplete and not included in the total zone count

age class as estimated previously for Indian Ocean yellowfin tuna (Farley et al. 2021). The final age, hereafter simply called age, of each fish was calculated by summing the age components estimated in the 3 steps.

2.3. Otolith preparation and radiocarbon analyses

Extraction of the early-growth portion of the 30 sub-adult and adult yellowfin tuna otoliths selected for age validation were performed following a series of steps. First, otoliths were embedded with Epofix resin, and the nucleus was identified under the microscope. Then, transverse sections between 1.8 and 2 mm thick were cut using an IsoMet low-speed saw while ensuring that the nucleus was centered within the section. Transverse sections were polished with a series of grinding and polishing films moistened with ultrapure water to ensure a smooth surface and enhance visibility of the growth bands. Sections were glued onto a sample plate using Crystalbond thermoplastic glue (Crystalbond 509, Buehler). Otoliths were cored, and the early-growth portion was isolated using a high-resolution New Wave Research Micro-Mill System consisting of an automated drill with a microscope and imaging system controlled by computer software. The targeted portion (Fig. 2A) was assumed to have been deposited during the first 1.5 yr of life, based on previous measurements of otoliths of age-1 and age-2 yellowfin tuna identified by modal progression analysis, and ensured the minimum sample weight for radiocarbon assays. A 300 mm diameter carbide bit (Gebr. Brasseler) was used over a pre-programmed template (Fig. 2), repeating the path from both sides of the transverse section until the desired portion was isolated as a solid chunk. The isolated material was weighed to the nearest 0.1 mg. For each otolith, a minimum of 3.0 mg of otolith material was collected in glassine weighing paper. All otoliths were digitally photographed at each step to record the methods used and ensure that the isolated otolith portion corresponded to the material deposited during the period 0–1.5 yr. The date of sample formation (i.e. the date best corresponding to when the extracted material analyzed for ^{14}C was deposited) was calculated as the catch date of fish collection minus the decimal age estimated by direct ageing, plus 0.75 (half of the mean extracted portion).

The extracted otolith material from the 30 age-validation samples and the whole otoliths from the 17 reference samples (yellowfin tuna of age-0 and age-1) were submitted to Beta Analytics for ^{14}C assay with accelerator mass spectrometry (AMS). AMS assays also provided carbon stable isotope ($\delta^{13}C$) values, which were used to correct for isotopic fractionation effects and provide information on the source of the carbon. Radiocarbon values are subsequently reported as $\Delta^{14}C$, which is the per mil (‰) deviation of the sample from the radiocarbon concentration of 19th-century wood, corrected for sample decay prior to 1950 according to methods outlined by Stuiver & Polach (1977). The mean standard deviation of the individual radiocarbon assays was about 2.7‰.

2.4. Reference ^{14}C chronologies

Tropical surface waters are the main habitat of yellowfin tuna during the first year of life, making coral records representative of the region inhabited by this species during the juvenile period. From the compilation of coral $\Delta^{14}C$ records in the Indian Ocean presented by Raj et al. (2022), 2 coral records were initially selected as reference chronologies to augment the known-age yellowfin tuna otolith data set: (1) the coral record from Watamu, off the Kenyan coast (Grumet et al. 2002), and (2) the coral record from Kadmat Island, west of the Indian continent (Raj & Bhushan 2021) (Fig. 1). The first was selected due to the geographic proximity to our region of interest, but this record ends in 1987 (Fig. 3A) and does not overlap with samples from the current study (estimated birth years from 2004 to 2018; see Section 3), so was not considered further. The coral $\Delta^{14}C$ record from Kadmat Island, while farther from our study location, ranges from 1977 to 2014 and therefore was selected to extend the otolith reference series to overlap with our study period (Fig. 3). To determine if the known-age otolith $\Delta^{14}C$ values (Table 1) and the Kadmat coral record yielded similar decline rates, the slopes of the coral and otolith records were statistically compared using a generalized linear model (GLM). Specifically, a GLM was fit to the reference data set with $\Delta^{14}C$ as the response variable, year as a covariate, reference material (coral or otolith) as a factor, and an interaction term between year and reference material, where a statistically significant interaction term would indicate different $\Delta^{14}C$ decline rates for the coral and otolith data. After verifying that the decline slopes of Kadmat corals and known-age otoliths were similar ($p > 0.05$), 2 different reference chronologies were considered for the age validation: the combination of corals and known-age otoliths ranging from 2000 to 2019 (Fig. 4A), and the record of known-age reference otoliths from 2006 to 2019 (Fig. 4B).

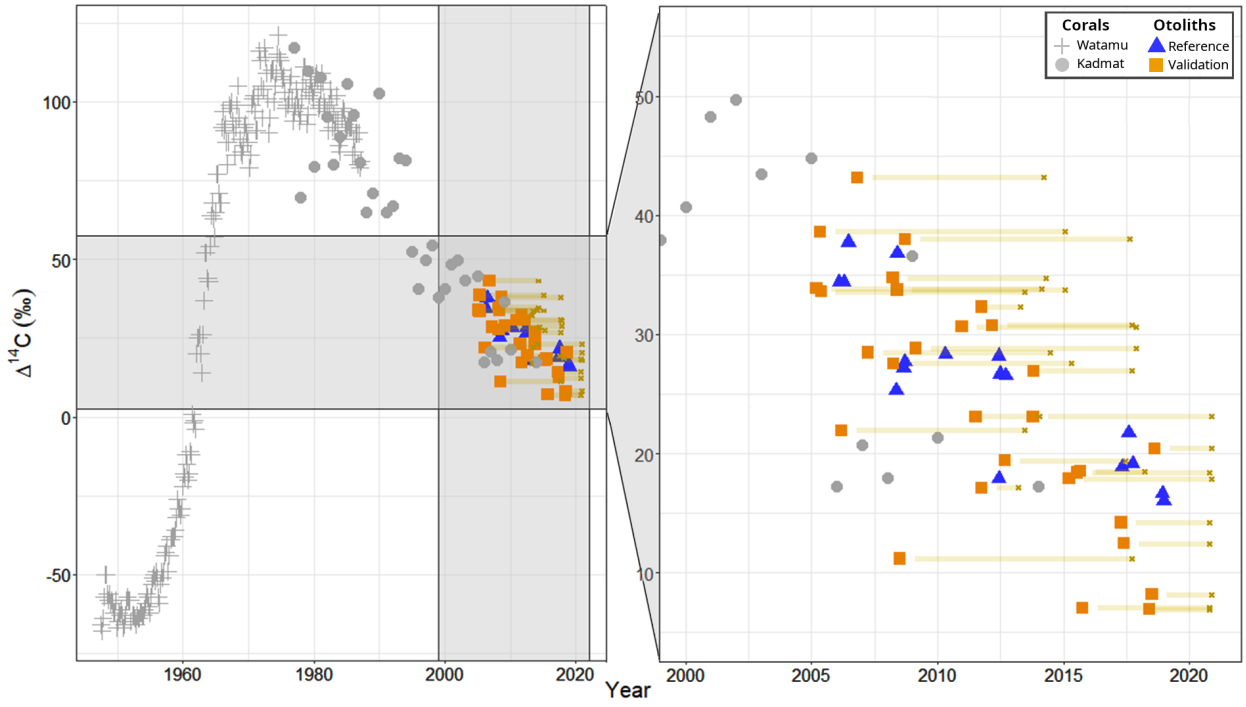

Fig. 3. Bomb $\Delta^{14}C$ variation versus year of formation for corals (grey), known-age reference otoliths (blue), and validation otoliths (orange) after back-calculating birth years from catch dates (crosses) and age estimates (horizontal lines). Coral records are from the western (Watamu, Kenya) and northern (Kadmat Island) Indian Ocean (Grumet et al. 2002, Raj et al. 2022)

2.5. Statistical analysis

Assumptions for normality and homogeneity of variance for the $\Delta^{14}C$ reference and otolith validation data sets were tested with a Shapiro-Wilk test and *F*-test, respectively. Significance levels were set at 95%. After confirming the assumptions of normality and homoscedasticity (Shapiro-Wilk normality test $p > 0.05$ for both reference and validation samples; *F*-test, $p > 0.05$), a GLM was used to evaluate if the decline in $\Delta^{14}C$ was similar for the reference chronology and otolith validation data sets. Like in the previous section, a GLM was fit to the whole data set with $\Delta^{14}C$ as the response variable, year of formation as a covariate, class of data (reference or validation) as a factor, and an interaction term between year and class. If the age estimates for the validation otolith samples were biased (e.g. the growth bands were not formed annually, or else were not being counted correctly when they had become compressed with age), then the estimated year of early growth formation would be incorrect and the $\Delta^{14}C$ decline curve for the validation data would be statistically significantly different from (and thus not be aligned with) the reference chronology decline curve. Thus, the slopes and intercepts of the reference and validation data were compared to determine if the $\Delta^{14}C$ decline curves were significantly different.

Residuals for the validation fish (calculated as measured $\Delta^{14}C$ minus predicted $\Delta^{14}C$ from the reference chronology decline curve) were used to look for patterns with age. The relationship between residuals and age was analyzed by fitting a linear regression, and Pearson correlation was used to test if there was a trend component in the relationship. Equality of variances in the residuals by age was tested using the Goldfeld-Quandt test, after first ordering the residuals by fish age. To assess possible effects of consistent biases in the age estimates on the residual pattern, simulations were carried out in which age estimates were shifted by ±1 and 2 yr. The resulting $\Delta^{14}C$ data with shifted birth years were then projected on the reference curve, and the residual sum of squares (RSS) values were compared among the simulations. This was done using both reference chronologies. All statistical analyses were carried out with R software (version 4.0.3).

3. RESULTS

3.1. Direct vs. ^{14}C-based age estimates

The direct age estimates of the sub-adult and adult validation otoliths ranged from 2.2 to 10.5 yr old,

Table 1. Decimal year of otolith formation, $\Delta^{14}C$ values with associated SE (analytical uncertainty in the measurement), and catch locations of known-age yellowfin tuna otoliths included in the regional reference data set and sub-adult and adult yellowfin tuna otoliths used for validation. Note that the catch location in some cases is approximate

Birth year	$\Delta^{14}C$	SE	Otolith class	Direct age estimate (yr)	Latitude (°N)	Longitude (°E)
2005.8	34.37	2.35	Reference	0.6	−0 to 20	40 to 60
2005.8	34.37	2.35	Reference	0.9	−0 to 20	40 to 60
2006.1	37.72	2.49	Reference	0.8	−0 to 20	40 to 60
2007.6	25.26	2.07	Reference	1.6	−6.6	55.0
2007.7	36.82	2.1	Reference	1.5	−6.6	55.0
2008.2	27.18	2.34	Reference	1.0	−7.4	55.0
2008.3	27.69	2.47	Reference	0.9	−7.4	55.0
2009.7	28.33	2.08	Reference	1.3	−5.9	58.5
2011.7	28.2	2.08	Reference	1.6	−15.8	43.4
2011.7	17.89	2.06	Reference	1.4	−10.1	58.5
2011.8	26.67	2.08	Reference	1.5	−15.8	43.4
2012.3	26.54	2.33	Reference	0.8	−10.1	58.5
2016.7	18.9	2.32	Reference	1.3	−20.8	55.2
2017.2	21.7	2.07	Reference	0.8	−7.5	54.5
2017.4	19.16	1.93	Reference	0.6	−0.7	53.3
2018.6	16.62	1.93	Reference	0.6	−2.5	54.3
2018.7	15.99	1.93	Reference	0.5	−2.5	54.3
2005.2	33.85	2.22	Validation	9.7	−3.3	44.6
2005.3	38.62	2.1	Validation	10.5	0.4	56.0
2005.4	33.59	2.09	Validation	8.8	−2.1	48.5
2006.2	21.95	2.84	Validation	8.0	−0.4	48.6
2006.8	43.16	2.64	Validation	8.1	−8.7	54.4
2007.2	28.46	2.73	Validation	8.0	−4.7	47.8
2008.2	34.75	2.48	Validation	6.8	−8.7	52.9
2008.2	27.56	2.21	Validation	7.8	−19.1	41.8
2008.4	33.72	2.09	Validation	7.4	−4.0	63.7
2008.5	11.19[a]	2.3	Validation	10.0	−21.2	50.0
2008.7	37.98	2.1	Validation	9.7	−19.1	53.9
2009.1	28.84	2.34	Validation	9.5	−23.0	55.1
2011.0	30.64	2.73	Validation	7.7	−20.5	54.4
2011.5	23.1	2.58	Validation	3.3	−5.6	59.1
2011.7	32.31	2.74	Validation	2.3	−18.6	42.2
2011.8	17.13	2.18	Validation	2.2	−15.8	43.4
2012.2	30.77	2.21	Validation	6.3	−18.0	54.5
2012.7	19.41	2.83	Validation	5.6	−20.5	54.0
2013.8	23.1	2.2	Validation	7.8	2.9	51.6
2013.8	26.93	2.34	Validation	4.7	−22.8	49.1
2015.2	17.89	2.19	Validation	6.4	2.9	51.6
2015.5	18.4	2.19	Validation	6.0	1.0	60.0
2015.7	18.52	2.19	Validation	3.3	−37.0	21.0
2015.7	7.05	2.29	Validation	5.8	1.0	60.0
2017.3	14.22	2.82	Validation	4.3	1.0	59.5
2017.4	12.45	2.17	Validation	4.1	7.0	59.6
2018.4	6.92	2.16	Validation	3.1	7.0	59.6
2018.5	8.18	2.67	Validation	3.1	7.4	60.7
2018.6	20.43	2.58	Validation	3.0	5.3	57.0

[a]Measurement was determined to be an outlier based on the residuals

resulting in back-calculated birth years from 2005 to 2018 (Table 1).

The whole otoliths from known-age (age-0 and age-1) yellowfin tuna had $\Delta^{14}C$ values between 15.99 and 37.72‰ (Table 1). The decline of $\Delta^{14}C$ though time observed in known-age reference otoliths corresponded well with the reference coral records during the period 2000–2019 (Fig. 3). There was no significant difference ($p > 0.05$) in the slope of the linear relationship of $\Delta^{14}C$ vs. year of formation between coral time series and known-age reference otoliths during the period 2000–2019 (Table 2). The rates of decline of $\Delta^{14}C$ in the reference chronologies were 1.5‰ yr^{-1} for the combined otolith + coral record (Table 3, Fig. 4A) and 1.3‰ yr^{-1} for the reference otoliths only (Table 3, Fig. 4B). The early growth portions of the 30 validation otoliths were successfully extracted from the otolith sections, and $\Delta^{14}C$ results were obtained for all samples (i.e. from both the portions of the validation otoliths and from the whole reference otoliths). One of the measurements from the validation set was deemed a measurement error (value outside of the cutoff range of mean ± 3 SD) and excluded from further analyses. $\Delta^{14}C$ values of the validation otoliths ranged from 6.92 to 43.16‰ (± standard error from 2.1 to 2.8‰) covering a potential time range of 13 yr (Table 1).

Measured $\Delta^{14}C$ values from sub-adult and adult otolith early growth portions were projected to the estimated birth dates based on increment counting (presumed to be annually formed) converted to decimal ages. These data points aligned well with $\Delta^{14}C$ values of the reference time series (Fig. 3). No significant difference was found between the $\Delta^{14}C$ decline curves (slopes and intercepts) of the 2 reference chronologies considered and the sub-adult and adult validation otoliths (Table 3).

3.2. Analysis of residuals

An examination of the distribution of residuals (measured − predicted $\Delta^{14}C$) for the sub-adult and adult validation otoliths indicated no major departure from normality using either reference curve (Shapiro-Wilk test, $p > 0.05$). The mean of the residuals was negative for both reference

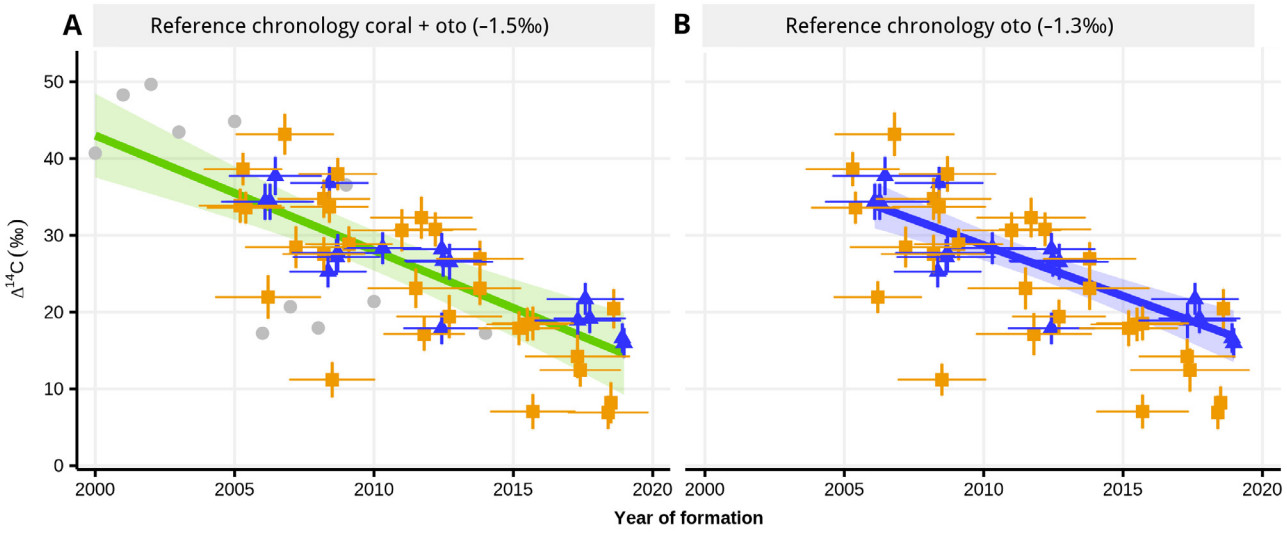

Fig. 4. Fitted linear regressions of the reference chronologies: (A) combination of corals + known-age otoliths from 2000 to 2019 (green) and (B) known-age otoliths from 2006 to 2019 (blue) overlaid with the validation samples (orange). Slopes of the linear regressions were −1.5 and −1.3‰ for A and B, respectively. Shaded area represents the 95% confidence interval. Vertical error bars represent ±1 SE of the $\Delta^{14}C$ measurements. The expected error in the year of formation due to the analytical uncertainty is estimated as SE/slope of the linear regression

curves (−1.36 and −2.34 using reference chronologies A and B, respectively), indicating that the direct age estimates were overestimated in comparison to the ^{14}C-derived ages estimates (Fig. 5). To check if the negative residuals were due to a systematic bias in annual growth zone counting, the existence of outliers within the residuals was determined (Grubb's outlier test). After removing 1 outlier, normality of residuals was improved, and the mean of the residuals approached 0 (−0.73 and −1.73 using reference chronologies of Fig. 4A,B, respectively). Based on the decline slopes of the reference chronologies used in this study, the residuals of $\Delta^{14}C$ represent an average difference of 0.5 and 1.3 yr between direct age estimates and radiocarbon-derived ages. Residuals of the sub-adult and adult validation otoliths were re-examined after excluding this 1 outlier sample, and revealed no relationship with age, either in terms of magnitude (evaluated by Pearson correlation test, correlation coefficients of 0.07 and 0.13 with associated p-values of 0.73 and 0.51 for reference chronologies of Fig. 4A,B, respectively) or variance (Goldfeld-Quandt test, p-values of 0.27 and 0.48 for reference chronologies of Fig. 4A,B, respectively) using either of the reference chronologies (Fig. 6).

Table 2. Results of the generalized linear model (GLM) performed on the reference data to test whether the regression lines of coral and known-age otolith $\Delta^{14}C$ declines have the same slope during the period 2000–2019, with Type as the factor representing the type of reference chronology (otolith or coral) and Year (year of formation of the carbonate) as a covariate. The interaction term (Year × Type) indicates whether the slopes are different, whereas the term Type indicates whether the intercepts of the 2 time series are different. Significance codes: *** = 100%; . = 90%

GLM	Estimate	SE	*t*	p	
Intercept	4879.3	947.2	5.2	<0.001	***
Year	−2.4	0.5	−5.1	<0.001	***
Type	−2189	1174	−1.9	0.075	.
Year × Type	1.1	0.6	1.9	0.074	.

Table 3. Results of the generalized linear models (GLMs) performed to test whether the reference chronologies and validation otoliths have the same slope, with Class as the factor representing the category of sample (reference or validation) and Year (year of formation) as a covariate. The interaction term (Year × Class) indicates whether the slopes are different, whereas the term Class indicates whether the intercepts of the 2 groups are different. Significance code: *** = 100%

	Estimate	SE	*t*	p	
GLM (coral + otolith reference)					
Intercept	3037.8	454.3	6.7	<0.001	***
Year	−1.5	0.2	−6.6	<0.001	***
Class	699.3	715.2	0.99	0.33	
Year × Class	−0.3	0.4	−0.99	0.33	
GLM (otolith reference)					
Intercept	2690.3	631.7	4.3	0.0001	***
Year	−1.3	0.3	−4.2	0.0001	***
Class	811.9	808.9	1.0	0.32	
Year × Class	−0.4	0.4	−1.0	0.32	

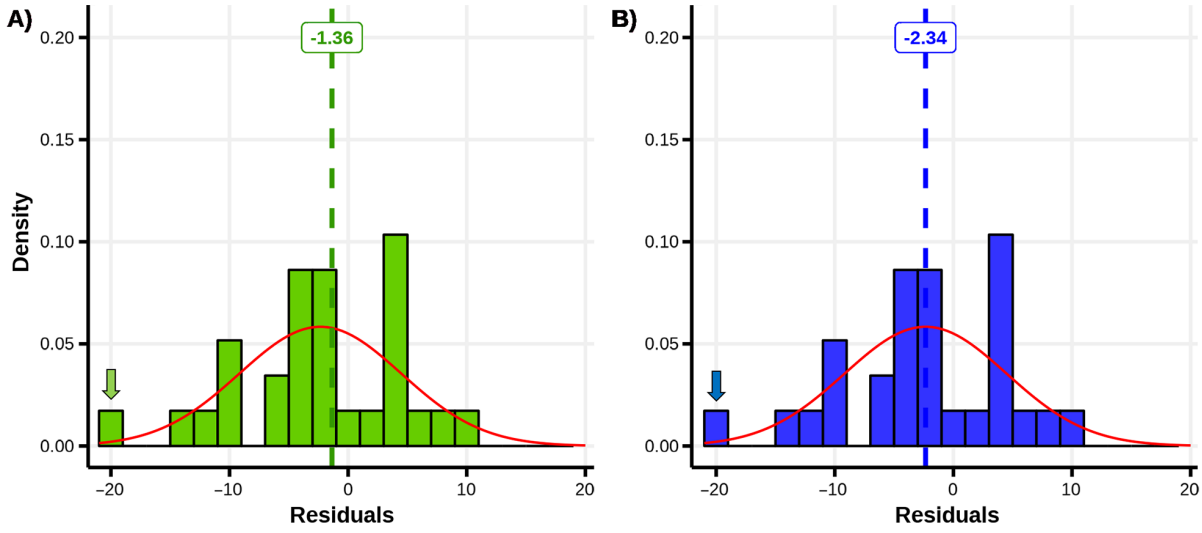

Fig. 5. Distribution and fitted normal distributions of residuals (measured − predicted $\Delta^{14}C$) using the reference chronologies: (A) corals + known-age otoliths (green) and (B) known-age otoliths only (blue). The dashed line denotes the mean values of the residuals. The arrow indicates the sample identified as an outlier

This indicates no systematic bias in the direct age estimates compared to age estimates inferred by the 2 $\Delta^{14}C$ reference curves, because if a systematic ageing error was present, the magnitude and/or the variance with age would be increased. The distribution of residuals appears normally distributed and centered close to zero, although there is some indication of a small negative bias (Fig. 6, right panel).

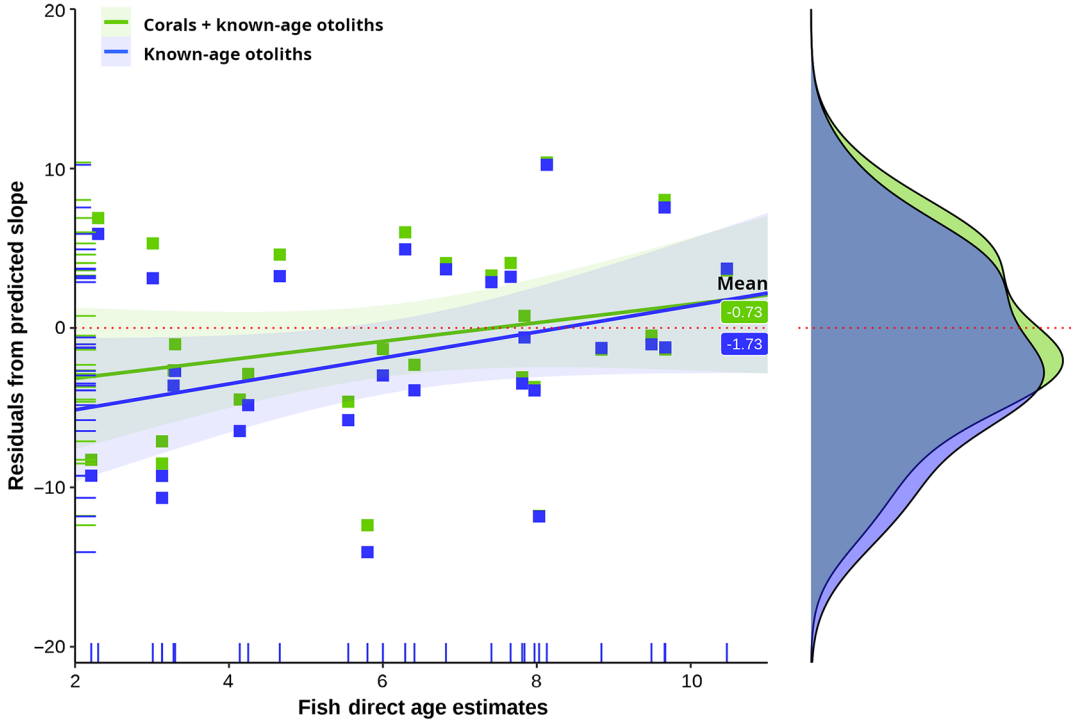

Fig. 6. Relationship between direct age estimates and residuals of $\Delta^{14}C$ (measured − predicted) in sub-adult/adult yellowfin tuna after excluding the outlier sample. Predicted slopes were estimated using (green) corals + known-age otoliths, and (blue) known-age otoliths (solid line = fitted linear model, and grey shaded area = 95% confidence interval). Means of the residuals were −0.73 and −1.73 using reference chronologies from Fig. 4A,B, respectively. Residuals <0 indicate that direct age estimates are higher than the radiocarbon-based ages. Dotted red line represents the horizontal reference line at zero. Right panel: density plot of residuals after excluding the outlier sample

3.3. Age bias analysis

The age bias analysis was performed by simulating overestimation and underestimation of the direct age estimates by shifting ±1 and 2 yr after excluding the outlier identified above. Results showed that the minimum RSS value was reached with the original age estimates (with no ageing error) using the coral + otolith reference chronology (RSS of 938), whereas shifted age estimates resulted in RSS values ranging from 940 to 1312. Instead, using the known-age otolith reference chronology, minimum RSS was attained when age estimates were shifted by −1 yr (RSS of 1006). RSS values of the age-bias analysis are reported in Table 4. The age-bias simulation study corroborates that direct age estimates coincide with radiocarbon-derived estimates when using the combined coral–otolith reference chronology, but differences of 1 yr arise when the known-age otolith time-series is used as the reference chronology.

4. DISCUSSION

4.1. Age validation of yellowfin tuna from the Indian Ocean

Analysis of the $\Delta^{14}C$ revealed that the age growth increments being counted are indeed annual. The year of formation of the otolith early growth portion (estimated by combining annual increment counts and otolith size measurements on the thin sections) were consistent with the radiocarbon reference chronologies, supporting the age estimation criteria presented by Farley et al. (2021). Both the slope and intercept of the regression line were indistinguishable between the validation and reference curves, confirming that on average, validation otoliths showed a good fit to the reference curve. The age validation of yellowfin tuna has been reported for the Atlantic Ocean (Andrews et al. 2020) and the Pacific Ocean (Andrews et al. 2022). Here, we extend the utility of the approach geographically and applied to the age validation of yellowfin tuna from the western Indian Ocean. Based on the current $\Delta^{14}C$ age validation, maximum age for yellowfin tuna from the Indian Ocean is at least 10.5 yr, similar to maximum ages reported by previous studies in this ocean (Shih et al. 2014, Farley et al. 2021), but lower than maximum validated ages of 18 and 13 yr found in the Atlantic and Pacific Oceans, respectively (Andrews et al. 2020, 2022). Given that the largest yellowfin tuna included in this study was close to the maximum sizes recorded for the Indian Ocean (Artetxe-Arrate et al. 2021), the maximum age validated here is likely close to the maximum age of the whole Indian Ocean population.

An analysis of the residuals for the validation data set identified an outlier. It is unlikely that age overestimation was the reason for the misalignment of this outlier with the reference curve, since the estimated age based on growth zone counting was 10 yr (with SFL of 170.5 cm) and the ^{14}C-derived age was '0'. After excluding this outlier datapoint, the absolute mean of the residuals decreased substantially; however, the mean was still negative with either reference curve, indicating that direct age estimates were higher than ^{14}C-derived ages. On average, the differences between the direct age estimates and radiocarbon-derived ages were 0.5 and 1.3 yr (using the reference chronologies of Fig. 4A,B, respectively), indicating that the age validation is highly sensitive to the selection of an appropriate reference chronology. While the low $\Delta^{14}C$ values departing from the 95% confidence interval of the regression line may be interpreted as age overestimations, they may be partially explained by the inadvertent inclusion of otolith material deposited during later stages, an artifact that often occurs during sample preparation (e.g. Ishihara et al. 2017). This occurrence may explain the low $\Delta^{14}C$ values found in some of the sub-adult and adult otoliths compared to the reference curve. The anomalously low otolith $\Delta^{14}C$ values can also be explained by residence in very deep or upwelled waters, although yellowfin tuna mostly inhabit the surface mixed layer above the thermocline (Song et al. 2008).

Table 4. Summary residual sum of squares (RSS) from predicted decline slopes of the age-bias simulation study where the direct age estimates were intentionally increased and decreased by 1 and 2 yr after excluding 1 outlier. Decline slopes were predicted using 2 different reference chronologies: combination of corals + known-age otoliths; and known-age otoliths. Lowest RSS values for each of the reference chronologies used are represented in **bold**

	Age-bias applied (yr)				
	0	+1	−1	+2	−2
Coral + otolith reference 2000–2019	**938**	1062	940	1312	1067
Otolith reference 2006–2019	1086	1263	**1006**	1538	1025

4.2. Limitations of the current age validation

The decline of the bomb radiocarbon signal in the Indian Ocean after ~1980 is less steep than the period

of increasing bomb signal and has a wide dispersion of $\Delta^{14}C$ values, both of which limit age validation. Precision of the age validation would be improved using archived otoliths from adult yellowfin tuna with birthdates coinciding with the period of increasing ^{14}C. Unfortunately, after intense research, we were unable to locate any archived otoliths from this region.

Another limitation of the yellowfin tuna age validation presented here is the reference chronology data set used for validation. One of the considerations relevant in applying $\Delta^{14}C$ chronologies to fish age validation is the selection of an appropriate reference $\Delta^{14}C$ chronology that represents the same habitat of the species of interest. In the Indian Ocean, $\Delta^{14}C$ reference chronologies in the literature were limited. The coral record used here from the northern Indian Ocean (Raj et al. 2022) was geographically distant from the capture area of the yellowfin tuna used in our study and may not represent the environment inhabited by these tunas in their first year and a half of life. However, the declining $\Delta^{14}C$ slopes of this coral time series and the known-age yellowfin tuna otoliths were statistically indistinguishable, supporting that age validation could be performed using a combined coral and otolith reference chronology. The otolith-only and the combined coral-otolith reference chronologies considered in this study were similar but slightly less steep than those reported in the eastern Indian Ocean (Gao et al. 2021), Pacific Ocean (Andrews et al. 2016, 2020), and Gulf of Mexico (Barnett et al. 2018). Variations in the $\Delta^{14}C$ depletion rates among regions are frequently related to local oceanography and biogeochemical cycling (Mahadevan 2001). It must be noted that the amount of coral data available for the study period was low, and both reference chronologies tested here were highly sensitive to outliers. Moreover, a reference $\Delta^{14}C$ chronology with a narrow prediction interval is particularly useful for quick-growing fish species with relatively short lifespans (Shervette et al. 2021), which is the case for yellowfin tuna. The reference chronologies considered here had wide prediction intervals, hindering the level of accuracy of the age validation. The age validation of yellowfin tuna and other species living in a similar habitat would greatly benefit from incorporating new reference samples and developing a robust reference curve for the western Indian Ocean. The $\Delta^{14}C$ record of known-age otoliths presented here extends the previous coral record from the northern and western Indian Ocean until 2019, data that can be used to validate age estimation for fishes from the same region.

4.3. Implications for management of yellowfin tuna in the Indian Ocean

The age validation of yellowfin tuna from the Indian Ocean presented here contributes to the expanding knowledge of age and growth of the species. The misspecification of growth, natural mortality, and reproductive parameters can strongly impact scientific advice informing the management measures adopted (Mangel et al. 2013, Carvalho et al. 2021). For example, the improved estimation of fish ages and growth models for western Pacific bigeye tuna has contributed to enhancing the management of this important stock (Farley et al. 2017). Moreover, the age-specific natural mortality is an important parameter in characterizing the productivity of a stock, and it is closely related to the maximum age (Hoyle et al. 2023). The stock assessment of Indian Ocean yellowfin tuna in 2021 was developed using 2 alternative growth curves estimated from tagging data and otolith readings (Fu et al. 2021). Statistical diagnostics applied to assessment models indicated that certain combinations of growth and other biological parameters were not compatible with observations, and suggested model misspecification and bias on the estimated productivity (Merino et al. 2022). Mortality estimates of the recent yellowfin tuna assessment in the Atlantic Ocean were derived from an age validation study (Andrews et al. 2020, Urtizberea et al. 2020, Pacicco et al. 2021). Hence, the current study confirming that the maximum validated age for the yellowfin tuna from the Indian Ocean is at least 10.5 yr, and improved growth models (Farley et al. 2021) are expected to reduce the uncertainties of Indian Ocean yellowfin tuna stock assessments and, hence, help improve the management of this important stock.

5. CONCLUSIONS

The current study is the first to use otolith $\Delta^{14}C$ to validate age estimates of a tropical tuna species in the Indian Ocean. The findings presented here confirm that increments in otoliths of yellowfin tuna from the Indian Ocean are formed annually, and this is a further step towards reducing uncertainties in the age-structured stock assessment models. The maximum validated age from this study was 10.5 yr. These results will increase confidence in the length-at-age relationship and mortality estimates used in the stock assessment of Indian Ocean yellowfin tuna, a stock that supports a valuable fishery, which is currently undergoing a recovery plan, in the Indian Ocean. The

accuracy of the age validation would benefit from the analysis of greater numbers and a longer time series of reference otoliths from known-age tuna or other species inhabiting the same region of the Indian Ocean. This age validation would also be improved by incorporating otoliths of adult yellowfin tuna with birthdates coinciding with the $\Delta^{14}C$ incline, as the accuracy of the age validation largely depends on the slope of the linear regression. The $\Delta^{14}C$ data presented here extends the available post-peak $\Delta^{14}C$ record from the western Indian Ocean and offers the opportunity of an age validation to fish species with relatively short lifespans occupying the same habitat as yellowfin tuna.

Acknowledgements. We thank the European Union and the FAO/IOTC for financial support to develop the collaborative project GERUNDIO (Contract No. 2020/SEY/FIDTD/IOTC – CPA 345335). We also thank the members of the consortium for their support through the project. Otoliths used for this study were collected within the GERUNDIO project or were part of the collection of samples available from the Indian Ocean Tuna Commission (IOTC), derived from the PSTBS-IO (GCP/INT/233/EC – Population structure of IOTC species in the Indian Ocean) and Indian Ocean Tuna Tagging Program (IOTTP) projects. This work could not have been carried out without the contribution of I. Krug, I. Onandia, and many anonymous fishermen/fisherwomen who provided otoliths of tropical tuna over the years. We are grateful to the Seychelles Fishing Authority for facilitating access to sample collection and processing in their laboratories. The views expressed herein can in no way be taken to reflect the official opinion of the European Union. This document is contribution no. 1205 from AZTI, Marine Research, Basque Research and Technology Alliance (BRTA).

LITERATURE CITED

Andrews AH, Ashford JR, Brooks CM, Krusic-Golub K and others (2011a) Lead radium dating provides a framework for coordinating age estimation of Patagonian toothfish (*Dissostichus eleginoides*) between fishing areas. Mar Freshw Res 62:781–789

Andrews AH, Kalish JM, Newman SJ, Johnston JM (2011b) Bomb radiocarbon dating of three important reef-fish species using Indo-Pacific $\Delta^{14}C$ chronologies. Mar Freshw Res 62:1259–1269

Andrews AH, Choat JH, Hamilton RJ, DeMartini EE (2015) Refined bomb radiocarbon dating of two iconic fishes of the Great Barrier Reef. Mar Freshw Res 66:305–316

Andrews AH, DeMartini EE, Eble JA, Taylor BM, Lou DC, Humphreys RL (2016) Age and growth of bluespine unicornfish (*Naso unicornis*): a half-century life-span for a keystone browser, with a novel approach to bomb radiocarbon dating in the Hawaiian Islands. Can J Fish Aquat Sci 73:1575–1586

Andrews AH, Humphreys RL, Sampaga JD (2018) Blue marlin (*Makaira nigricans*) longevity estimates confirmed with bomb radiocarbon dating. Can J Fish Aquat Sci 75: 17–25

Andrews AH, Pacicco A, Allman R, Falterman BJ, Lang ET, Golet W (2020) Age validation of yellowfin (*Thunnus albacares*) and bigeye (*Thunnus obesus*) tuna of the northwestern Atlantic Ocean. Can J Fish Aquat Sci 77: 637–643

Andrews AH, Okamoto K, Satoh K, Roupsard F, Welte C, Farley J (2022) Final report on bomb radiocarbon age validation for yellowfin and bigeye tunas in the WCPO (Project 105)–2022. Western and Central Pacific Fisheries Commission. WCPFC-SC18-2022/SA-IP-14

Artetxe-Arrate I, Fraile I, Marsac F, Farley JH and others (2021) A review of the fisheries, life history and stock structure of tropical tuna (skipjack *Katsuwonus pelamis*, yellowfin *Thunnus albacares* and bigeye *Thunnus obesus*) in the Indian Ocean. Adv Mar Biol 88:39–89

Barnett BK, Thornton L, Allman R, Chanton JP, Patterson WF III (2018) Linear decline in red snapper (*Lutjanus campechanus*) otolith $\Delta^{14}C$ extends the utility of the bomb radiocarbon chronometer for fish age validation in the Northern Gulf of Mexico. ICES J Mar Sci 75:1664–1671

Broecker W, Peng TH (1982) Tracers in the sea. Lamont-Doherty Earth Observatory, Eldigio Press, Palisades, NY

Campana SE (1997) Use of radiocarbon from nuclear fallout as a dated marker in the otoliths of haddock, *Melanogrammus aeglefinus.* Mar Ecol Prog Ser 150:49–56

Campana SE (1999) Chemistry and composition of fish otoliths: pathways, mechanisms and applications. Mar Ecol Prog Ser 188:263–297

Campana SE (2001) Accuracy, precision and quality control in age determination, including a review of the use and abuse of age validation methods. J Fish Biol 59: 197–242

Campana SE, Jones CM (1998) Radiocarbon from nuclear testing applied to age validation of black drum, *Pogonias cromis.* Fish Bull 96:185–192

Campana SE, Natanson LJ, Myklevoll S (2002) Bomb dating and age determination of large pelagic sharks. Can J Fish Aquat Sci 59:450–455

Carvalho F, Winker H, Courtney D, Kapur M and others (2021) A cookbook for using model diagnostics in integrated stock assessments. Fish Res 240:105959

DeMartini EE, Andrews AH, Howard KG, Taylor BM, Lou DC, Donovan MK (2018) Comparative growth, age at maturity and sex change, and longevity of Hawaiian parrotfishes, with bomb radiocarbon validation. Can J Fish Aquat Sci 75:580–589

Druffel EM, Linick TW (1978) Radiocarbon in annual coral rings of Florida. Geophys Res Lett 5:913–916

Druffel EM, Suess HE (1983) On the radiocarbon in banded corals: exchange parameters and net transport of $^{14}CO_2$ between atmosphere and surface ocean. J Geophys Res 88:1271–1280

Eveson P, Million J, Sardenne F, Le Croizier G (2015) Estimating growth of tropical tunas in the Indian Ocean using tag-recapture data and otolith-based age estimates. Fish Res 163:58–68

FAO (2020) The state of world fisheries and aquaculture 2020. Sustainability in action. Food and Agriculture Organization of the United Nations, Rome

Farley J, Eveson P, Krusic-Golub K, Sanchez C and others (2017) Project 35: Age, growth and maturity of bigeye tuna in the western and central Pacific Ocean. WCPFC-SC13-2017/SA-WP-01. https://meetings.wcpfc.int/node/10188

Farley J, Krusic-Golub K, Eveson P, Clear N and others (2020) Age and growth of yellowfin and bigeye tuna in

the western and central Pacific Ocean from otoliths. WCPFC-SC16-2020/SA-WP-02. https://meetings.wcpfc.int/node/11692

Farley J, Krusic-Golub K, Eveson P, Lastra-Luque P and others (2021) Estimating the age and growth of yellowfin tuna (*Thunnus albacares*) in the Indian Ocean from counts of daily and annual increments in otoliths. IOTC-2021-WPTT23-05_Rev1

Fu D, Urtizberea A, Cardinale M, Methot RD, Hoyle DS, Merino G (2021) Preliminary Indian Ocean yellowfin tuna stock assessment 1950–2020 (Stock Synthesis). IOTC Working Party on Tropical Tunas 21. IOTC-2021-WPTT23-12. https://www.iotc.org/documents/WPTT/2302/12

Gao P, Quian N, Zhou L, Liu K (2021) Decadal changes of seawater radiocarbon in the eastern tropical Indian Ocean and their oceanographic implications. J Mar Syst 213:103453

Grumet NS, Guilderson TP, Dunbar RB (2002) Watamu Reef, Kenya coral radiocarbon data. IGBP PAGES/World Data Center for Paleoclimatology Data Contribution Series # 2002-084. NOAA/NGDC Paleoclimatology Program, Boulder CO

Grumet TS, Duffy PB, Wickett ME, Caldeira K, Dunbar RB (2005) Intrabasin comparison of surface radiocarbon levels in the Indian Ocean between coral records and three-dimensional global ocean models. Global Biogeochem Cycles 19:GB2010

Guilderson TP, Caldeira K, Duffy PB (2000) Radiocarbon as a diagnostic tracer in ocean and carbon cycle modelling. Global Biogeochem Cycles 14:887–902

Hoyle SD, Williams AJ, Minte-Vera CV, Maunder M (2023) Approaches for estimating natural mortality in tuna stock assessments: application to global yellowfin tuna stocks. Fish Res 257:106498

IOTC (Indian Ocean Tuna Commission) (2023) Report of the 25th Session of the IOTC Scientific Committee. Online, 5–9 December 2022. IOTC-2022-SC25-R[E]. https://iotc.org/documents/WPTT/2501/RE

Ishihara T, Abe O, Shimose T, Takeuchi Y, Aires-da-Silva A (2017) Use of post-bomb radiocarbon dating to validate estimated ages of Pacific bluefin tuna, *Thunnus orientalis*, of the North Pacific Ocean. Fish Res 189:35–41

ISSF (International Seafood Sustainability Foundation) (2023) Status of the world fisheries for tuna. Tech Rep 2023–01. ISSF, Pittsburgh, PA

Kalish JM (1989) Otolith microchemistry: validation of the effects of physiology, age and environment on otolith composition. J Exp Mar Biol Ecol 132:151–178

Kalish JM (1993) Pre- and post-bomb radiocarbon in fish otoliths. Earth Planet Sci Lett 114:549–554

Kalish JM, Johnston JM, Gunn JS, Clear NP (1996) Use of the bomb radiocarbon chronometer to determine age of southern bluefin tuna *Thunnus maccoyii.* Mar Ecol Prog Ser 143:1–8

Kalish JM, Johnston JM, Smith DC, Morison AK, Robertson SG (1997) Use of the bomb radiocarbon chronometer for age validation in the blue grenadier *Macruronus novaezelandiae.* Mar Biol 128:557–563

Kastelle CR, Kimura DK, Goetz BJ (2008) Bomb radiocarbon age validation of Pacific ocean perch (*Sebastes alutus*) using new statistical methods. Can J Fish Aquat Sci 65: 1101–1112

Kastelle CR, Helser T, TenBrink T, Hutchinson C, Goetz B, Gburski C, Benson I (2020) Age validation of four rockfishes (genera *Sebastes* and S*ebastolobus*) with bomb-produced radiocarbon. Mar Freshw Res 71:1355–1366

Krusic-Golub K, Ailloud L (2022) Evaluating otolith increment deposition rates in bigeye tuna (*Thunnus obesus*) and yellowfin tuna (*T. albacares*) tagged in the Atlantic Ocean. Fish Bull 121:1–16

Lessa R, Duarte-Neto P (2004) Age and growth of yellowfin tuna (*Thunnus albacares*) in the western equatorial Atlantic, using dorsal fin spines. Fish Res 69:157–170

Lu D, Lin Q, Zhu J, Zhang F (2023) Effects of aging uncertainty on the estimation of growth functions of major tuna species. Fishes 8:131

Mahadevan A (2001) An analysis of bomb radiocarbon trends in the Pacific. Mar Chem 73:273–290

Mangel M, MacCall AD, Brodziak J, Dick EJ, Forrest RE, Pourzard R, Ralston SA (2013) Perspective on steepness, reference points, and stock assessment. Can J Fish Aquat Sci 70:930–940

Melvin GD, Campana SE (2010) High resolution bomb dating for testing the accuracy of age interpretations for a short-lived pelagic fish, the Atlantic herring. Environ Biol Fishes 89:297–311

Merino G, Urtizberea A, Fu D, Winker H and others (2022) Investigating trends in process error as a diagnostic for integrated fisheries stock assessments. Fish Res 256: 106478

Michel RL, Linick TW (1985) Uptake of bomb-produced carbon-14 by the Weddell Sea. Meteoritics 20:423–434

Morales-Nin B (2000) Review of the growth regulation processes of otolith daily increment formation. Fish Res 46: 53–67

Murua H, Rodríguez-Marín E, Neilson J, Farley J, Juan-Jordá MJ (2017) Fast versus slow growing tuna species — age, growth, and implications for population dynamics and fisheries management. Rev Fish Biol Fish 27:733–773

Nydal R, Lovseth K (1983) Tracing bomb ^{14}C in the atmosphere 1962–1980. J Geophys Res 88:3621–3642

Pacicco AE, Allman RJ, Lang ET, Murie DJ, Falterman BJ, Ahrens R, Walter JF (2021) Age and growth of yellowfin tuna in the U.S. Gulf of Mexico and Western Atlantic. Mar Coast Fish 13:345–361

Punt AE, Castillo-Jordán C, Hamel OS, Cope JM, Maunder MN, Ianelli JN (2021) Consequences of error in natural mortality and its estimation in stock assessment models. Fish Res 233:105759

Raj H, Bhushan R (2021) Spatial and temporal changes in bomb radiocarbon in the northern Indian Ocean. J Environ Radioact 237:106680

Raj H, Bhushan R, Banerji US, Muruganantham M, Shah C, Nambiar R, Dabhi AJ (2022) Air–sea CO_2 exchange rate in the northern Indian Ocean based on coral radiocarbon records. Appl Geochem 137:105208

Sanchez PJ, Pinsky JP, Rooker JR (2019) Bomb radiocarbon age validation of Warsaw grouper and snowy grouper. Fisheries 44:524–533

Sardenne F, Dortel E, Le Croizier G, Million J and others (2015) Determining the age of tropical tunas in the Indian Ocean from otolith microstructures. Fish Res 163:44–57

Shervette VR, Overly KE, Rivera-Hernández JM (2021) adiocarbon in otoliths of tropical marine fishes: reference $\Delta^{14}C$ chronology for north Caribbean waters. PLOS ONE 16:e0251442

Shih CL, Hsua CC, Chenb CY (2014) First attempt to age yellowfin tuna, *Thunnus albacares*, in the Indian Ocean, based on sectioned otoliths. Fish Res 149:19–23

Song LM, Zhang Y, Xu LX, Jiang WX, Wang JQ (2008) Environmental preferences of longlining for yellowfin tuna (*Thunnus albacares*) in the tropical high seas of the Indian Ocean. Fish Oceanogr 17:239–253

Stuiver M, Polach H (1977) Discussion: Reporting of ^{14}C Data. Radiocarbon 19:355–363

Then AY, Hoenig JM, Hall NG, Hewitt DA (2015) Evaluating the predictive performance of empirical estimators of natural mortality rate using information on over 200 fish species. ICES J Mar Sci 72:82–92

Ticina V, Katavic I, Grubisic L (2007) Growth indices of small northern bluefin tuna (*Thunnus thynnus, L.*) in growth-out rearing cages. Aquaculture 269:538–543

Urtizberea A, Cardinale M, Winker H, Methot R and others (2020) Towards providing scientific advice for Indian Ocean yellowfin in 2020. IOTC-2020-WPTT22(AS)-21

Wexler JB, Margulies D, Masuma S, Tezuka N and others (2001) Age validation and growth of yellowfin tuna, *Thunnus albacares*, larvae reared in the laboratory. Inter Am Trop Tuna Comm Bull 22:52–91

Editorial responsibility: Konstantinos Stergiou, Thessaloniki, Greece
Reviewed by: 3 anonymous referees

Submitted: August 2, 2023
Accepted: February 6, 2024
Proofs received from author(s): April 10, 2024